

Journal of Materials Chemistry A

Accepted Manuscript



This is an *Accepted Manuscript*, which has been through the Royal Society of Chemistry peer review process and has been accepted for publication.

Accepted Manuscripts are published online shortly after acceptance, before technical editing, formatting and proof reading. Using this free service, authors can make their results available to the community, in citable form, before we publish the edited article. We will replace this *Accepted Manuscript* with the edited and formatted *Advance Article* as soon as it is available.

You can find more information about *Accepted Manuscripts* in the [Information for Authors](#).

Please note that technical editing may introduce minor changes to the text and/or graphics, which may alter content. The journal's standard [Terms & Conditions](#) and the [Ethical guidelines](#) still apply. In no event shall the Royal Society of Chemistry be held responsible for any errors or omissions in this *Accepted Manuscript* or any consequences arising from the use of any information it contains.

ARTICLE

Microwave-synthesized poly(ionic liquid) particles: a new material with high electrorheological activity

Cite this: DOI: 10.1039/x0xx00000x

Yuezhen Dong^a, Jianbo Yin^{a,*} and Xiaopeng Zhao^a,Received 00th January 2012,
Accepted 00th January 2012

DOI: 10.1039/x0xx00000x

www.rsc.org/

Hydrophobic poly(ionic liquid) particles are synthesized by a microwave-assisted dispersion polymerization and their electro-responsive characteristic are investigated as new water-free polyelectrolyte-based electrorheological (ER) system. Structure characterization shows the poly(ionic liquid) particles are uniform microspheres with narrow size distribution of $\sim 1.8 \mu\text{m}$ and low density of $\sim 1.62 \text{ g/cm}^3$. Under electric fields, the fluid of poly(ionic liquid) particles in silicone oil shows low current density but high ER activity including small off-field viscosity, large field-induced shear stress and storage modulus, and stable flow curves in wide shear rate region. The ER effect increases with particle content. The typical shear stress is $\sim 2500 \text{ Pa}$ at 4 kV/mm and 100 s^{-1} , which is ~ 30 times as high as the off-field shear stress. Dielectric spectra analysis indicates that the high ER activity can be attributed to strong dielectric polarizability and adequate polarization response induced by the high-density of cation/anion parts in poly(ionic liquid) particles. The ER activity also depends on the type of cation/anion parts.

Introduction

Smart materials can respond to external stimuli by transmitting their physical and chemical properties.¹⁻³ Electrorheological (ER) fluids, consisting of polarizable particles in insulating oil, are considered to be one of the most interesting and important smart materials with electrically tunable rheology.⁴ They have potential uses as electrical-mechanical interfaces for the active-control of various devices because of technical advantages, such as rapid response time, reversibility, and low power consumption.⁵ However, the practical utilization of ER fluids is still limited by some shortcomings, such as low electro-responsive efficiency, large leaking current, poor dispersion stability, and thermal instability.

Many efforts have been devoted to develop high-performance ER material systems. Among various ER systems, polyelectrolyte is considered to be one of the most promising candidates due to the low density, low abrasive, and relatively high ER activity.⁶ The well-known polyelectrolyte ER materials include poly(lithium methacrylate), poly(sodium styrene sulfonate), and other polyether salts or ion-exchange resins.^{6,7} Under external electric fields, the ER effect of the polyelectrolyte is considered to be related to the ionic mobility-induced interfacial or surface polarization. As a dry powder, however, the metal ions in the polyelectrolyte are strongly bound by the carboxylate or sulfonate groups. Thereby, the conventional polyelectrolyte particles often need to absorb a quantity of water or other solvents to promote ionic mobility and thus activate ER effect. Unfortunately, the addition of

water is fraught with the problems associated with the evaporation or leaching and large leaking current density, which largely limit technical applications.

As a new kind of polymer electrolyte, poly(ionic liquid)s (PILs) have attracted significant attentions recently because PILs not only inherit some unique properties of ionic liquids (e.g. low vapor pressures, highly thermostability and nonflammability) but also possess well-defined solid morphologies and mechanical property that are inaccessible by ILs.⁸⁻¹¹ PILs can be prepared by the direct polymerization of ionic liquid monomer which has polymerizable groups. The polymerization inevitably reduces the ionic motion and, as a result, the ionic conductivity of PILs is relatively too low for commercial ion-conducting applications.¹⁰ However, the reduced conductivity of PILs is suitable for electro-responsive ER fluid applications because ER materials belong to leaking dielectric systems. Importantly, different from conventional polyelectrolyte, to make ions locally move in the PILs does not need the presence of water and other solvents. At the same time, PILs contain high-density of cation/anion parts and therefore have strong dipoles.¹¹ These characters endow PILs with potential as new water-free polyelectrolyte-based ER system showing large dielectric polarization and highly electro-responsive behavior. To the best of our knowledge, however, no reports are available on the electro-responsive ER properties of PILs. Herein, we use a facile microwave-assisted dispersion polymerization to prepare hydrophobic PIL particles and investigate their electro-responsive characteristic as new water-

free polyelectrolyte-based ER system by rheological tests. Different from conventional polyelectrolyte-based ER system, the PIL particles are demonstrated to possess low current density but high ER activity in absence of any activators. Dielectric spectra analysis indicates that the high ER activity can be attributed to the strong dielectric polarization of PILs induced by the intrinsic high-density of cation/anion parts.

Experimental section

Materials

Reagent grade 2,2'-azobis(isobutyronitrile) (AIBN, Sinopharm Chemical Reagent Co. Ltd. of China) was purified by recrystallization in methanol. Poly(vinylpyrrolidone) (PVP, K-30, weight-average molecular weight: 3.6×10^5 g/mol, BASF), ethanol (Sinopharm Chemical Reagent Co. Ltd. of China), [2-(methacryloyloxy)ethyl]trimethylammonium chloride solution ([MTMA]-Cl, 80 wt % in water, Aldrich), and lithium bis(trifluoromethane sulfonyl)imide (Li[TFSI], 99%, Aldrich) were used as received.

Fabrication of P[MTMA][TFSI] particles

First, the ionic liquid monomer [2-(methacryloyloxy)ethyltrimethylammonium bis(trifluoromethanesulfonyl)imide] ([MTMA][TFSI]) was prepared by mixing aqueous solutions of 4.400 g [MTMA]Cl and 4.600 g Li[TFSI] according to ref [12]. After phase separation, washing with distilled water, and vacuum drying, the oily ionic liquid monomer of [MTMA][TFSI] was obtained. Then, 2.000 g [MTMA][TFSI], 0.144 g PVP and 0.020 g AIBN were added in ethanol. After stirring for 30 min at room temperature, the resulting solution was treated at temperature of 70 °C, stirring rate of 120 rpm, and pressure of 20 psi for 7 h with a CEM Explorer microwave synthesis instrument. Finally, the precipitate was separated, washed with ethanol and vacuum dried to obtain resulting poly[2-(methacryloyloxy)ethyltrimethylammonium bis(trifluoromethanesulfonyl)imide] (P[MTMA][TFSI]) particles.

Characterization

The morphology was observed by scanning electron microscopy (SEM, Hitachi TM-300). The crystal structure was determined by powder x-ray diffraction pattern (XRD, Philips X'Pert Pro). The thermal transformation of samples was determined by the thermogravimetric analyzer (TGA, Netzsch STA449F3) with heating rate of 10 °C/min within 30–800 °C in air. The chemical group was determined by the Fourier transform infrared spectra (FT-IR, JASCO FT/IR-470 Plus). ^1H nuclear magnetic resonance (^1H NMR) measurement was carried out at room temperature using a Bruker DPX-400 spectrometer operating at 400 MHz. DMSO- d_6 was used as solvent. The DC conductivity (σ_{DC}) of samples was measured

by a two-point method (Keithley 6517B) on the P[MTMA][TFSI] film.

Preparation of ER fluids

The P[MTMA][TFSI] particles were further vacuum dried for 48 h and then mixed into silicone oil (Dielectric constant of ~ 2.7 , viscosity of 50 mPa·s, density of 0.96 g/cm 3 at 25 °C) by mechanical stirring and ultrasonic to form uniform fluids. The volume fraction of particles in fluids was defined by the ratio of particle volume to total fluid volume. The density of PIL particles was measured by a pycnometer filled with silicone oil (density of 0.96 g/cm 3 at 25 °C). To decrease the effect of porosity on density, the pycnometer was placed in an ultrasonic cleaning bath and connected to a vacuum pump. After ultrasonic under reduced pressure for 10 min, the density was measured.

Dispersion stability measurements

The dispersion stability of particles in fluids was characterized by sedimentation test at room temperature. A graduated flask was used to record the height of phase separation between the particle-rich phase and the relatively clear oil-rich phase as a function of aging time. The sedimentation ratio was defined by the height percentage of particle-rich phase relative to the total fluid height. The higher the sedimentation ratio was, the better the dispersion stability was.

Rheological measurements

The ER structures of dispersed particles formed between two electrodes were observed by an optical microscopy (Nikon ALPHAPHOT-2). The ER properties of fluids were measured by a stress-controlled rheometer (Thermal-Haake RS600) with a parallel plate system with diameter of 35 mm and gap of 1.0 mm, DC high-voltage generator, oil bath system, and PC computer. Steady shear flow curves of shear stress-shear rate were measured by the controlled shear rate (CSR) mode within 0.1 - 1000 s $^{-1}$ at room temperature. Before each measurement, we presheared the fluids for 60 s at 300 s $^{-1}$ and then applied electric fields for 30 s to ensure the formation of equilibrium gap-spanning ER structures of dispersed particles before shearing. In the dynamic oscillation test, the sweep test of modulus as a function of stress at a constant frequency of 1.0 Hz was initially conducted to find a linear viscoelastic region, and then the dynamic viscoelastic moduli were measured as a function of frequency at a stress in the linear viscoelastic region. The electric fields were applied for 60 s prior to applying sweeping.

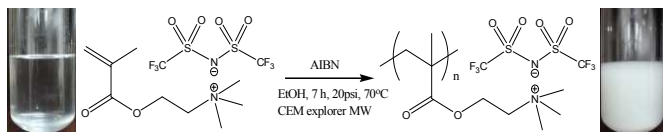
Dielectric measurements

The dielectric properties of particles in fluids were measured by an impedance analyzer (HP 4284A) using a measuring fixture (HP 16452A) for liquids. 1 V of bias electrical potential was applied during measurement. Thus, no chain formation within

fluids was induced and, as a result, we could well understand the interfacial polarization.

Results and discussions

[MTMA][TFSI] monomer is polymerized in ethanol by microwave-assisted dispersion polymerization (see Scheme 1). AIBN is used as the initiator. PVP is used as the steric stabilizer to avoid the agglomerate of polymeric particles during growth process in polymerization reaction and thus favors the growth of PIL particles with narrow size distribution.¹³ The reaction temperature is 70 °C and pressure is 20 psi. At the same time, an in-situ stirring with moderate rate of 120 rpm is applied. Finally, the particles are separated, washed and vacuum dried to obtain resulting P[MTMA][TFSI] particles.



Scheme 1 Preparation of P[MTMA][TFSI] particles by microwave-assisted dispersion polymerization.

Fig. 1 shows the morphology of P[MTMA][TFSI] particles by SEM. It is found that the P[MTMA][TFSI] particles are well-defined microspheres with narrow size distribution of ~ 1.8 μm (see inset in Fig. 1). Besides reactant and polymerization processing conditions, using the microwave irradiation as heat source can induce fast and effectively homogeneous heating of the monomers, which favors the homogeneous formation of growing centers of polymer chains in the initial stage and results in the reduction of side reactions. As a result, the product is cleaner and monodisperse.¹⁴

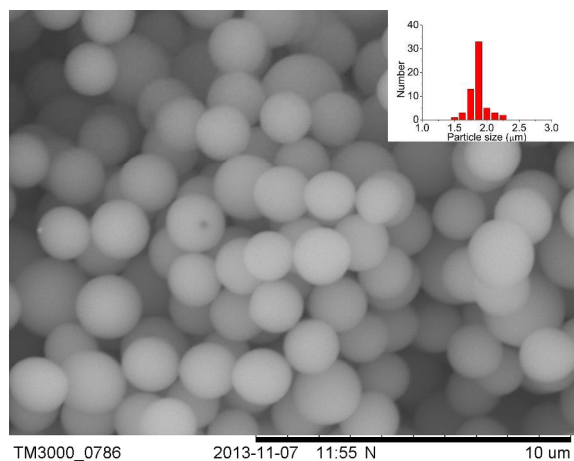


Fig. 1 SEM image and size distribution (inset) of P[MTMA][TFSI] particles.

The XRD pattern in Fig. 2(a) shows that the P[MTMA][TFSI] particles are amorphous. The ^1H NMR spectrum (DMSO- d_6 , 400 MHz, ppm) of P[MTMA][TFSI] particles in Fig. 2(b) shows the peaks at 4.30 (br, 2H), 3.65 (br, 2H) and 3.16 (s, 9H) due to the proton in the P[MTMA][TFSI]

monomeric unit and the peaks at 2.2-0.2 (m, 5H) due to the proton in the backbone of P[MTMA][TFSI] macromonomer unit.¹⁵ The sharp singlet at 2.50 ppm and 3.35 ppm are attributed to the solvent DMSO- d_6 and rudimental H_2O in the solvent. No peaks corresponding to [MTMA][TFSI] monomer means that the polymerization is complete. The FT-IR spectrum of P[MTMA][TFSI] particles in Fig. 2(c) shows that there are not only the characteristic bands corresponding to the P[MTMA] cation part (CH_3 stretching vibration at 3057 cm^{-1} , CH_2 stretching vibration at 2992 cm^{-1} , CH_2 variable-angle vibration at 1483 cm^{-1} , etc.) but also the characteristic bands corresponding to the [TFSI] anion part ($\text{S}(\text{=O})_2$ asymmetrical stretching vibration at 1353 cm^{-1} , $\text{C}=\text{O}$ stretching vibration at 1735 cm^{-1} , CF_3 stretching vibration at 1198 cm^{-1} , $\text{S}=\text{O}$ symmetrical stretching vibration at 1139 cm^{-1} , $\text{S}=\text{O}$ stretching vibration at 1055 cm^{-1} , etc.).¹⁶ The TGA trace in Fig. 2(d) shows that the P[MTMA][TFSI] particles have good thermal stability. The onset of degradation is at about $320\text{ }^\circ\text{C}$.

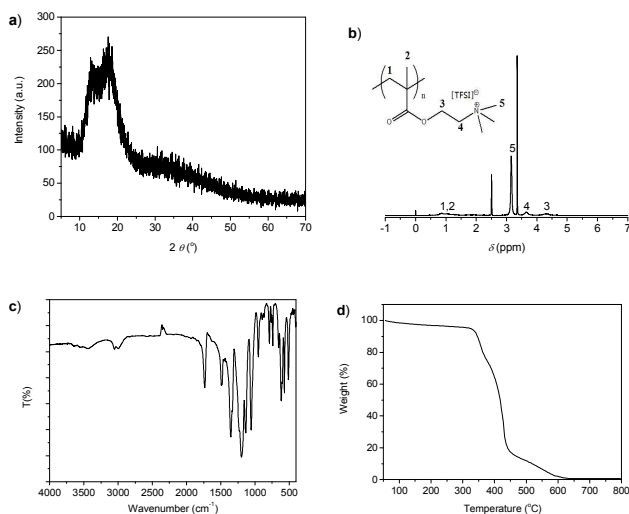


Fig. 2 (a) XRD pattern, (b) ^1H NMR spectrum, (c) FT-IR spectrum, and (d) TGA curve of P[MTMA][TFSI] particles.

The conductivity (σ_{DC}) of P[MTMA][TFSI] particles is $\sim 2.2 \times 10^{-9}\text{ S/cm}$, which is significantly lower compared to that of [MTMA][TFSI] monomer. It indicates that the polymerization has restrained the long-range mobility of the ions because the P[MTMA] cation part is covalently attached to the polymer backbone and the [TFSI] anion part has been reduced mobility due to the higher viscosity in the solid-like polymeric particles. However, the conductivity range of P[MTMA][TFSI] particles is suitable for ER fluid application according to the conduction model.¹⁷

Due to hydrophobic nature, the P[MTMA][TFSI] particles are easy to disperse in silicone oil and the resulting fluid shows good dispersion stability. After aging for one month without stirred, the sedimentation ratio of the PILs-based ER fluid is about 80%, which is significantly better than that of most of ER

fluids.⁴ This can be attributed to the low density ($\sim 1.62 \text{ g/cm}^3$) and hydrophobic nature of P[MTMA][TFSI] particles.

Under applied electric fields, the optical microscope in Fig. 3(a) shows that randomly dispersed P[MTMA][TFSI] particles rapidly contact each other and form gap-spanning dense fibrous structure between electrodes, indicating a good electro-response. This aligned fibrous structure, which is dominated by sufficient electrostatic interaction between P[MTMA][TFSI] particles, will provide a large resistance to the shear flow perpendicular to electric fields and thus enhance shear stress. Fig. 3(b) shows the real-time response of shear stress of the PILs-based ER fluid to applied electric fields when alternately turned on and off. It is found that, when the electric fields are applied, the shear stress of fluid increases instantaneously. The value of shear stress at 4.0 kV/mm is about 30 times as high as that of off-field shear stress. When the electric fields are removed, the shear stress drops rapidly back to the original level. As the electric field strength increases, the shear stress increases and the real-time response of shear stress is still reversible and reproducible, revealing good electro-responsive characteristic of the PILs-based ER fluid.

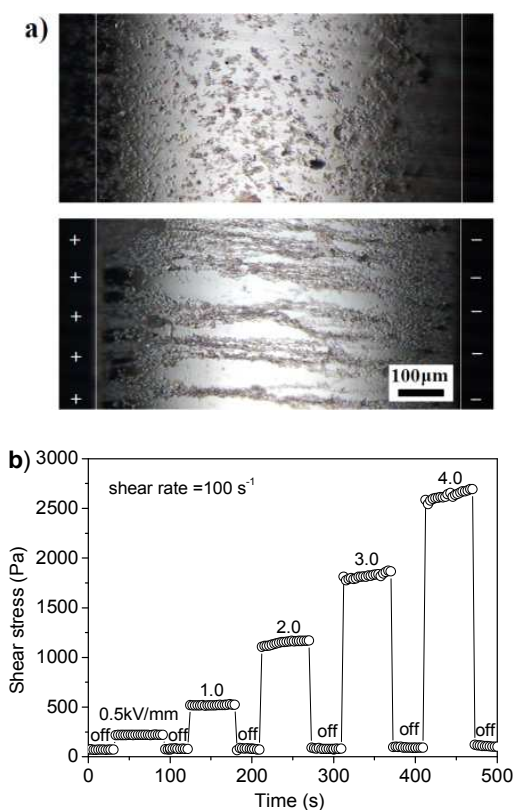


Fig. 3 (a) Optical photo of the ER fluid of P[MTMA][TFSI] particles without and with electric fields ($\phi = 3 \text{ vol}\%$, $T = 23^\circ\text{C}$); (b) Effect of switching the applied electric fields on the shear stress of the ER fluid of P[MTMA][TFSI] particles ($\phi = 28 \text{ vol}\%$, $T = 23^\circ\text{C}$).

Fig. 4(a) shows the flow curves of shear stress as a function

of shear rate for PILs-based ER fluid with particle content of 28 vol%. Before the application of electric fields, similar to many other particle suspensions, the PILs-based ER fluid behaves as a non-Newtonian fluid with shearing thin phenomenon but does not possess significant yield stress. The off-field viscosity is $\sim 0.29 \text{ Pa}\cdot\text{s}$ at 1000 s^{-1} , which is lower than that of most inorganic ER fluids, such as silica gel and zeolite at the same particle content.^{7a} This may be attributed to the low density of PIL particles. When the electric fields are applied, the fluid exhibits a strong increase in shear stress and a Bingham plastic behavior with the presence of a yield stress is observed at various electric field strengths. This indicates that the fluid has transformed from a liquid-like state into a solid-like state due to the formation of fibrous structure as shown in Fig. 3(a). As the electric field strength increases, the enhancement in shear stress is clear due to the increase of interparticle electrostatic interaction. For example, the electric field-induced shear stress is $\sim 2500 \text{ Pa}$ at 4.0 kV/mm and 100 s^{-1} , which is ~ 30 times as high as that at 0 kV/mm. The electric field-induced shear stress is $\sim 3010 \text{ Pa}$ at 4.0 kV/mm and 1000 s^{-1} , which is still ~ 10 times as high as that at 0 kV/mm.

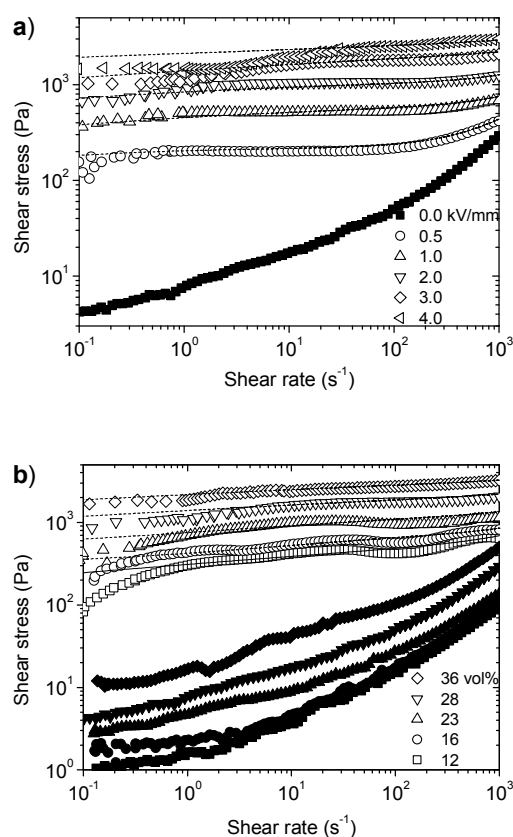


Fig. 4 (a) Flow curves of shear stress vs. shear rate for the ER fluid of P[MTMA][TFSI] particles under various electric fields ($\phi = 28 \text{ vol}\%$, $T = 23^\circ\text{C}$). Dash lines are fitting curves by CCJ model; (b) Flow curves of shear stress vs. shear rate for the ER fluid of P[MTMA][TFSI] particles with different particle contents ($E = 0 \text{ kV/mm}$ (solid symbol), 3.0 kV/mm (open symbol), $T = 23^\circ\text{C}$). Dash lines are fitting curves by CCJ model.

This PILs-based ER fluid also shows stable flow curves, where the shear stress keeps slight increase with the increasing of shear rate, rather than the shear stress decrease obviously with the increase of shear rate. It's known that the rheological behavior of ER fluids is related to the change (i.e. breaking and rebuilding) of field-induced particle chain structures under the simultaneous effect of both electric and shear fields, which is further dominated by the competition between the electric field-induced electrostatic interaction between particles and the shear field-induced hydrodynamic interaction.¹⁸ The electrostatic interaction is responsible for the rebuilding of particle chains and hinders the flow, while the hydrodynamic interaction tends to break particle chains and promotes the flow. The stable flow curve in wide shear rate region reflects that electric field-induced electrostatic interaction between PIL particles is so strong that it can effectively rebuild particle chains in the wide shear rate range. Fig. 4(b) shows the flow curves of shear stress vs. shear rate for different particle content of ER fluids. As the particle content increases, both off-field shear stress and electric field-induced shear stress of PILs-based ER fluid increase. The ER efficiency (defined by τ_E/τ_0 , where τ_E is shear stress with electric fields and τ_0 is shear stress without electric fields) reaches its maximum at moderate particle content of 20–30 vol%. At different particle contents, the fluid still maintains relatively stable flow curves in a wide shear rate region, which is useful for technological applications.¹⁹

Fig. 5 plots the dynamic yield stress (τ_d) as a function of electric field strength (E) and particle content (ϕ). τ_d is defined as the stress making ER fluids continuously flow, which is very important parameter used in designing electroactive devices where flow properties are essential.⁴ We use Cho–Choi–Jhon (CCJ) model,^{20,21} which is considered to be better to fit the flow curves of ER fluids compared to Bingham model, to fit the flow curves as shown in Fig. 4 and obtain τ_d values. The CCJ model is described by the equation (1) as below:

$$\tau = \frac{\tau_d}{1 + (t_2\dot{\gamma})^\alpha} + \eta_0 \left(1 + \frac{1}{(t_3\dot{\gamma})^\beta}\right) \dot{\gamma} \quad (1)$$

Here, τ_d is the dynamic yield stress, η_0 is the viscosity at infinite shear rate or at zero electric field, t_2 and t_3 are time constants used to describe the variation in the shear stress. The exponent α is related to the change in the shear stress at the low shear rate region, while β in the range of 0–1 is for the high shear rate region. As shown in Fig. 5(a), the dependence of dynamic yield stress on field strength follows by the power-law relation of $\tau_d \propto E^a$. The value of exponent a is 1.1–1.8 for different particle contents, which differs from that τ_d is proportional to the electric field strength E^2 predicted by the classic polarization model.²² This can be attributed to the fact that the polarization model treats dielectric particles as ideal point dipoles and thus the electrostatic interaction between dielectric particles is

treated as a dipole–dipole interaction only. However, in the factual ER fluids several factors, such as particle content, shape, multi-dispersion, nonlinear conductivity of oil, etc. often make it differ from 2.^{23–25} As the particle content increases, the value of exponent a decreases. The analogical phenomenon is also observed in other ER fluids.²³ Furthermore, the PILs-based ER fluid possess low current leakage (see inset in Fig. 5(a)). When the electric field strength is 4.0 kV/mm and the particle content is about 28 vol%, the current density is less than 25 $\mu\text{A}/\text{cm}^2$, which is lower than that of conventional water-activated polyelectrolyte-ER materials.^{6,7} The low current leakage also reflects that the polymerization has restrained the long-range mobility of the ions. As shown in Fig. 5(b), the correlation of dynamic yield stress on particle content follows by the power-law relation of $\tau_d \propto \phi^b$ (see Fig. 5(b)). The value of exponent b is 1.5–2.5 for different electric field strengths, which is larger than 1. This can be attributed to the fact that more compact ER structure has been formed with the increase of particle content, where the restriction of affine deformation leads to larger yield stress.²⁶ As the electric field strength increases, the value of exponent b decreases.

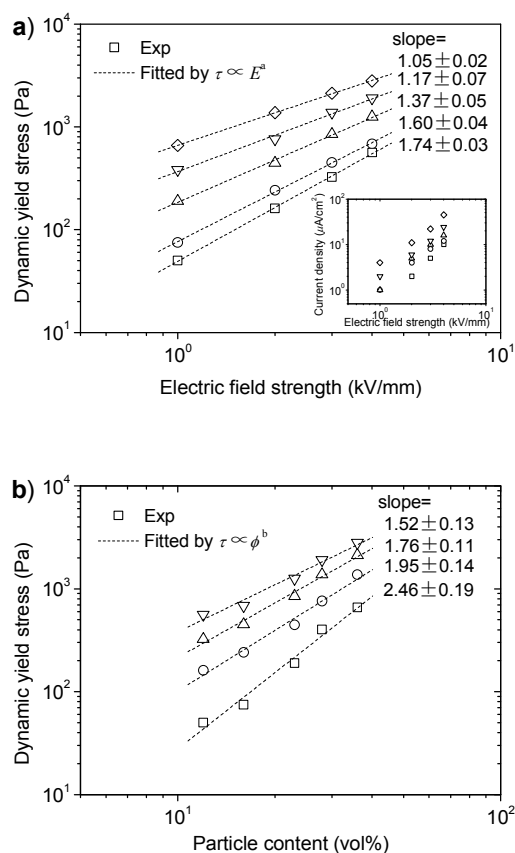


Fig. 5 (a) Dynamic yield stress and current density (inset) as a function of electric field strength for the ER fluid of P[MTMA][TFSI] particles ($\phi = 12$ vol% (\square), 16 (\circ), 23 (\triangle), 28 (∇), and 36 (\diamond), $T=23^\circ\text{C}$); (b) Dynamic yield stress as a function of particle content for the ER fluid of P[MTMA][TFSI] particles ($E=1.0$ kV/mm (\square), 2.0 (\circ), 3.0 (\triangle), 4.0 (∇), $T=23^\circ\text{C}$).

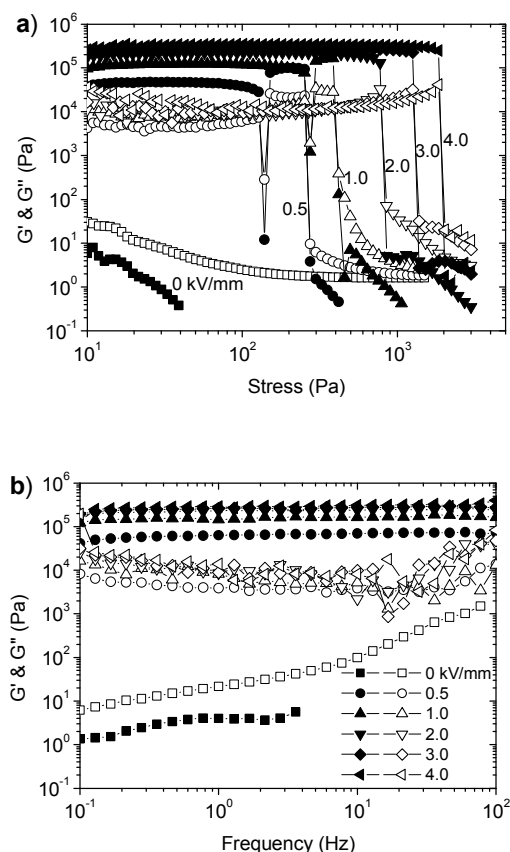


Fig. 6 (a) Stress amplitude dependence of storage modulus (G' , solid symbol) and loss modulus (G'' , open symbol) at the oscillation frequency of 1 Hz for the ER fluid of P[MTMA][TFSI] particles under various electric fields ($\phi = 28$ vol%, $T = 23^\circ\text{C}$); (b) Frequency dependence of storage modulus (G' , solid symbol) and loss modulus (G'' , open symbol) at the stress amplitude of 30 Pa for the ER fluid of P[MTMA][TFSI] particles under various electric fields ($\phi = 28$ vol%, $T = 23^\circ\text{C}$).

On the other hand, in the design of non-flowing smart devices, control of the pre-yield dynamic viscoelastic property of ER fluids is also important. Fig. 6(a) shows the shear storage modulus (G') and loss modulus (G'') of the PILs-based ER fluid as a function of stress amplitude at the frequency of 1 Hz. In the absence of electric fields, the fluid is liquid-like state according to larger G'' than G' . In the presence of electric fields, the fluid shows solid-like state according to the fact that G' is larger than G'' and G' remains constant, so-called linear viscoelastic behavior, before the stress amplitude exceeds the yield value. As the electric field strength increases, both G' and G'' increase and the linear viscoelastic region becomes broader, indicating increased solidity or solidification level. As the stress amplitude increases and exceeds the yield point, the shear moduli of fluid drops suddenly and the solidified fluid becomes a viscous fluid according to larger G'' than G' . In particular, unlike ER fluids based on polydispersible particles or elongated particles which often show a shoulder-like yield process due to complex ER

structuring transformation,^{5c,27} the decrease of shear moduli of PILs-based ER fluid is sudden. This may be related to the fact that the PIL particles are monodisperse spheres and thus the ER structuring transformation is relatively simple. Furthermore, it is also noted that the static yield stress obtained from Fig. 6(a) is slightly smaller than the dynamic yield stress in Fig. 5 at the same particle content. The similar result is also observed in other ER fluids and magnetorheological fluids.^{25,28} Fig. 6(b) shows the shear modulus of the PILs-based ER fluid as a function of frequency in the linear viscoelastic region. It is found that the PILs-based ER fluid is liquid-like state without electric fields. When electric fields are applied, G' is substantially larger than G'' , and G' remains nearly constant over a broad deformation frequency range, also indicating that the fluid has transformed into a solid-like state. As the electric field strength increases, both G' and G'' increase.

To understand the electro-responsive ER effect of PIL particles, we measure the dielectric properties of fluid. As shown in Fig. 7, the PILs-based ER fluid shows a clear dielectric dispersion or dielectric relaxation within measured frequency region, which can be attributed to the interfacial polarization of PIL particles in silicone oil. The Cole-Cole equation shown in the equation (2) is used to fit the dielectric data and to analyze the dielectric characteristic:

$$\varepsilon^* = \varepsilon' + i\varepsilon'' = \varepsilon_\infty + \frac{\varepsilon'_0 - \varepsilon_\infty}{1 + (j\omega\lambda)^{1-\alpha}} \quad (2)$$

Here, ε^* is a complex permittivity of suspension, ε'_0 and ε'_∞ are the limit values of the relative permittivity at the frequencies below and above the relaxation frequencies, respectively, ω is an angle frequency, λ is a dielectric relaxation time denoted by $\lambda = 1/(2\pi f_{\max})$ (where f_{\max} is the relaxation frequency defined by a local maximum of the dielectric loss factor ε''), and α is the scattering degree of relaxation time. $\Delta\varepsilon'$ ($\Delta\varepsilon' = \varepsilon'_0 - \varepsilon'_\infty$) is the achievable polarizability that is related to the electrostatic interaction between particles and λ is related to the rate of interfacial polarization of particles. It has been reported that, when the λ becomes smaller within an adequate range (10^2 - 10^5 Hz) and a larger $\Delta\varepsilon'$ is applied, higher stress enhancement or ER effect is achieved.²⁹ In the fitting result, the $\Delta\varepsilon'$ and λ values of PILs-based ER fluid are ~ 6.5 and ~ 0.00042 s, respectively. These suggest a large polarizability and an adequately rapid polarization response of PIL particles under an applied electric field, which provide effective evidences of the high ER activity. We consider that this large dielectric polarization may be mainly attributed to the unique cation/anion parts in PILs. On one hand, the high-density of cation/anion parts induce strong dipole under electric fields and thus enhance dielectric constant. On the other hand, the locally motion of [TFSI] anions in PIL particles induces an appropriate conductivity for adequate polarization response within an adequate range (10^2 - 10^5 Hz).

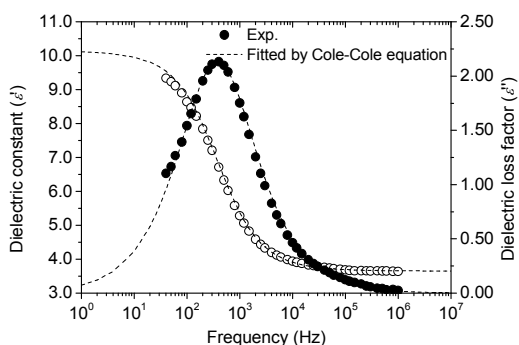


Fig. 7 Frequency dependence of dielectric constant (ϵ' , open points) and loss factor (ϵ'' , solid points) of the ER fluid of P[MTMA][TFSI] particles. ($\phi=28$ vol%, $T=23^\circ\text{C}$)

Finally, it is noted that the ER effect of PILs-based ER fluid depends on the type of cation/anion parts. Table 1 presents the dielectric and ER properties of several PILs-based ER fluids. Although the off-field viscosity (η_0) of ER fluid of P[MTMA][TFSI] is lower than that of ER fluid of P[EVI][TFSI] (poly[1-ethyl-3-vinylimidazolium bis(trifluoromethanesulfonylimide)]), the shear stress (τ_E) of the former is ~ 1750 Pa at shear rate of 100 s^{-1} and electric field of 3.0 kV/mm , which is significantly higher than that (~ 458 Pa) of the latter. This can be attributed to the fact that the P[MTMA][TFSI] with ammonium cations is more polar than P[EVI][TFSI] with imidazolium cations when their anions are same.^{9,30} However, the shear stress of ER fluid of P[MTMA][BF₄] (poly[2-(methacryloyloxy)ethyltrimethylammonium tetrafluoroborate]) is about ~ 1560 Pa at shear rate of 100 s^{-1} and electric field of 3.0 kV/mm , which is slightly lower than that of ER fluid of P[MTMA][TFSI]. This may be attributed to that the polarizability of P[MTMA][TFSI] is slightly higher than that of P[MTMA][BF₄].³¹ This also indicates that the cation parts attached with backbone may be more dominant to the dielectric and ER properties of PILs.

Table 1. Comparison of dielectric and ER properties for various PILs-based ER fluids ($\phi=28$ vol%, $T=23^\circ\text{C}$)

Material	ϵ'_0	ϵ'_∞	$\Delta\epsilon'$	λ/s	τ_E/Pa	$\eta_0/\text{Pa}\cdot\text{s}$
P[MTMA][TFSI]	10.1	3.6	6.5	0.00042	1750	0.29
P[EVI][TFSI]	6.8	3.2	3.6	-	458	0.39
P[MTMA][BF ₄]	9.2	3.5	5.7	0.00033	1560	0.48

Conclusions

In summary, by a facile microwave-assisted dispersion polymerization, we have synthesized uniform hydrophobic P[MTMA][TFSI] particles for use as a new water-free polyelectrolyte-based ER system. Due to low density of 1.62 g/cm^3 , the PILs-based ER fluid shows good dispersion stability. Different from conventional water-activated polyelectrolyte-

based ER system, the PILs-based ER fluid shows high ER activity in the absence of any activators. The typical shear stress at 100 s^{-1} and storage modulus of 28 vol% PILs-based ER fluid are ~ 2500 Pa and ~ 340000 Pa at 4.0 kV/mm . At the same time, the flow curves of fluid can maintain stable in the wide shear rate region. The PILs-based ER fluid also shows low leaking current density due to its water-free characteristic. According to the dielectric spectra analysis, the high ER activity of PILs can be attributed to strong dielectric polarizability and adequate polarization response induced by the intrinsic high-density of cation/anion parts. The type of cation/anion parts influences the dielectric polarization and ER activity of PILs. The present result suggests that PIL particles have large potential as new water-free polyelectrolyte-based ER system with high-performance due to their unique structure and property.

Acknowledgements

This work is supported by the Program for New Century Excellent Talents in University of China, National Natural Science Foundation of China (no. 51272214), and NPU Foundation for Fundamental Research (no. JC20120247).

Notes and references

^a Smart Materials Laboratory, Department of Applied Physics, Northwestern Polytechnical University, Xi'an 710129, P. R. China. Fax: 86 29 88491000; Tel: 86 29 88431662; E-mail: jbyin@nwpu.edu.cn

- J. R. Capadona, K. Shanmuganathan, D. J. Tyler, S. J. Rowan and C. Weder, *Science*, 2008, **319**, 1370
- K. Tsuchiya, Y. Orihara, Y. Kondo, N. Yoshino, T. Ohkubo, H. Sakai and M. Abe, *J. Am. Chem. Soc.*, 2004, **126**, 12282
- K. Isozaki, H. Takaya and T. Naota, *Angew. Chem. Int. Ed.* 2007, **46**, 2855
- (a) T. C. Hasley, *Science*, 1992, **258**, 761; (b) K. D. Weiss, J. D. Carlson and J. P. Coulter, *J. Intell. Mater. Syst. Struct.*, 1993, **4**, 13; (c) T. Hao, *Adv. Colloid Interface Sci.*, 2002, **97**, 1; (d) B. J. Park, F. F. Fang and H. J. Choi, *Soft Matter*, 2010, **6**, 5246; (e) J.-Y. Hong and J. Jang, *Soft Matter*, 2012, **8**, 3348.
- (a) Y. M. Han, P. S. Kang, K. G. Sung and S. B. Choi, *J. Intell. Mater. Syst. Struct.*, 2007, **18**, 1149; (b) X. Niu, M. Zhang, J. Wu, W. Wen and P. Sheng, *Soft Matter*, 2009, **5**, 576; (c) J. B. Yin, X. P. Zhao, L. Q. Xiang, X. Xia and Z. S. Zhang, *Soft Matter*, 2009, **5**, 4687; (d) P. Sheng and W. Wen, *Annu. Rev. Fluid Mech.*, 2012, **44**, 143; (e) H. Tang, K. Huang and R. Tao, *J. Intelligent Mater. Syst. Struct.*, 2011, **22**, 1673.
- (a) J. E. Stangroom, *G. B. Patent Specification* 1570234, 1980; (b) J. E. Stangroom, *U.S. Patent Specification* 4502973, 1985; (c) J. E. Stangroom, *G. B. Patent Specification* 2153372, 1985.
- (a) T. Hao, *Adv. Mater.*, 2001, **13**, 1847; (b) J. M. Ginder and S. L. Ceccin, *J. Rheol.*, 1995, **39**, 211; (c) H. Q. Xie, J. G. Guan, J. Shi and G. Q. Xie, *J. Appl. Polym. Sci.*, 1995, **58**, 951; (d) R. Bloodworth and E. Wendt, *Int. J. Mod. Phys. B*, 1996, **10**, 2951; (e) H. I. Unal, O. Agirbas and H. Yilmaz, *Colloids Surf. A*, 2006, **274**, 77.

- 8 J. Yuan, D. Mecerreyes and M. Antonietti, *Prog. Polym. Sci.*, 2013, **38**, 1009.
- 9 J. Tang, W. Sun, H. M. Radosz and Y. Shen, *Macromolecules*, 2005, **38**, 2037.
- 10 M. Dobbelin, I. Azcune, M. Bedu, A. R. de Luzuriaga, A. Genua, V. Jovanovski, G. Cabanero and I. Odriozola, *Chem. Mater.*, 2012, **24**, 1583.
- 11 J. Tang, M. Radosz and Y. Shen, *Macromolecules*, 2008, **41**, 493.
- 12 M. Tokuda, H. Minami, Y. Mizuta and T. Yamagami, *Macromol. Rapid Commun.*, 2012, **33**, 1130.
- 13 J. W. Kim and K. D. Suh, *Colloid Polym. Sci.*, 1988, **276**, 870.
- 14 F. Wiesbrock, R. Hoogenboom and U. S. Schubert, *Macromol. Rapid Commun.*, 2004, **25**, 1739.
- 15 X. Hu, J. Tang, A. Blasig, Y. Shen and M. Radosz, *J. Membrane Sci.*, 2006, **281**, 130.
- 16 M. Tokuda and H. Minami, *J. Colloid Interf. Sci.*, 2013, **398**, 120.
- 17 P. Atten, J. N. Foulc and N. Felici, *Int. J. Mod. Phys. B*, 1994, **8**, 2731.
- 18 M. Parthasarathy and D. J. Klingenberg, *Mater. Sci. Eng. R*, 1996, **17**, 57.
- 19 (a) R. Shen, X. Wang, Y. Lu, D. Wang, G. Sun, Z. Cao and K. Lu, *Adv. Mater.*, 2009, **21**, 4631; (b) Y. Cheng, K. Wu, F. Liu, J. Guo, X. Liu, G. Xu and P. Cui, *ACS Appl. Mater. Interfaces*, 2010, **2**, 621.
- 20 M. S. Cho, H. J. Choi and M. S. Jhon, *Polymer*, 2005, **46**, 11484.
- 21 Y. D. Liu, F. F. Fang and H. J. Choi, *Soft Matter*, 2011, **7**, 2782.
- 22 D. J. Klingenberg and C. F. Zukoski, *J. Chem. Phys.*, 1991, **94**, 6160.
- 23 Y. Otsubo, *Colloids Surf. A*, 1999, **153**, 459.
- 24 M. S. Cho, Y. H. Cho, H. J. Choi and M. S. Jhon, *Langmuir*, 2003, **19**, 5875.
- 25 J. B. Yin, X. P. Zhao, X. Xia, L. Q. Xiang and Y. P. Qiao, *Polymer*, 2008, **49**, 4413.
- 26 X. Tang, Y. Chen and H. Conrad, Structure and interaction force in a model magnetorheological materials. In: W. A. Bullough, *Electrorheological fluids, magnetorheological suspensions and associated technology*, World Scientific, Singapore, 1996.
- 27 J. B. Yin, X. Xia, X. X. Wang and X. P. Zhao, *Soft Matter*, 2011, **7**, 10978.
- 28 J. de Vicente, F. Vereda and J. P. Segovia-Gutierrez, *J. Rheol.*, 2010, **54**, 1337.
- 29 (a) H. Block, J. P. Kelly, A. Qin and T. Watson, *Langmuir*, 1990, **6**, 6; (b) F. Ikazaki, A. Kawai, K. Uchida, T. Kawakami, K. Edmura, K. Sakurai, H. Anzai and Y. Asako, *J. Phys. D: Appl. Phys.*, 1998, **31**, 336.
- 30 H. Tokuda, S. Tsuzuki, M. A. B. H. Susan, K. Hayamizu and M. Watanabe, *J. Phys. Chem. B*, 2006, **110**, 19593.
- 31 K. Nakamura, K. Fukao and T. Inoue, *Macromolecules*, 2012, **45**, 3850.